

Excitonic Effects in the Photoluminescence of C-Plane Polar AlGa_N Quantum Wells

Greg Rupper, Sergey Rudin, Gregory Garrett, and Meredith Reed

U. S. Army Research Laboratory, Adelphi, Maryland, USA, greg.rupper.ctr@mail.mil

Al_xGa_{1-x}N narrow quantum wells (QW) are important elements of deep-ultraviolet light emitting devices. Due to the large exciton binding energy there can be significant exciton effects in photoluminescence (PL) from AlGa_N even at room temperature. The exciton binding energy is reduced due to the strong polarization fields in c-plane quantum wells, screening from donor electrons and optically pumped carriers. In this work we model the PL from an AlGa_N QW with a partially ionized electron-hole gas in quasi-thermal equilibrium. The predicted radiative decay times are then compared to experimental results.

In order to accurately model a partially ionized electron-hole gas at relatively high densities of photo-excited electron-hole carriers and arbitrary temperature, we employed real-time Green's function formalism with self-energies evaluated in the self-consistent T-matrix approximation [1]. We included one conduction and one top hole band in the perturbation theory formalism. For the device modeled in this work (2.5nm Al_{0.45}Ga_{0.55}N QW with Al_{0.55}Ga_{0.45}N barriers strained to Al_{0.6}Ga_{0.4}N), the top hole band corresponds to the crystal-field split hole band and was approximated by an effective mass in the QW-plane and growth direction.

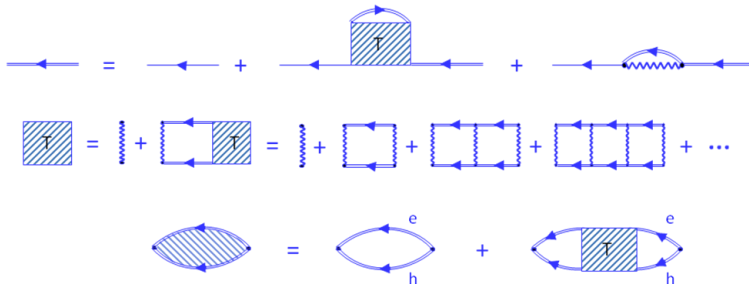


Fig. 1. Feynman diagrams for the QW optical susceptibility. The first line shows the self-energies included in the single particle propagator. The T-matrix (second line) includes the infinite Coulomb ladder diagrams and allows for excitonic effects. The third line shows the optical susceptibility.

The Feynman diagrams relevant for the evaluation of optical susceptibility of electron-hole plasma are shown in Fig. 1 and described in reference 1. The T-matrix includes the infinite Coulomb ladder diagram, and allows for excitonic effects in a theory that starts with free-particles. A statically screened Coulomb potential, evaluated in the plasmon-pole approximation, was used in place of the bare potential. The wave function in the growth direction includes the effects of the polarization field, and self-consistent density dependent screening of the polarization field.

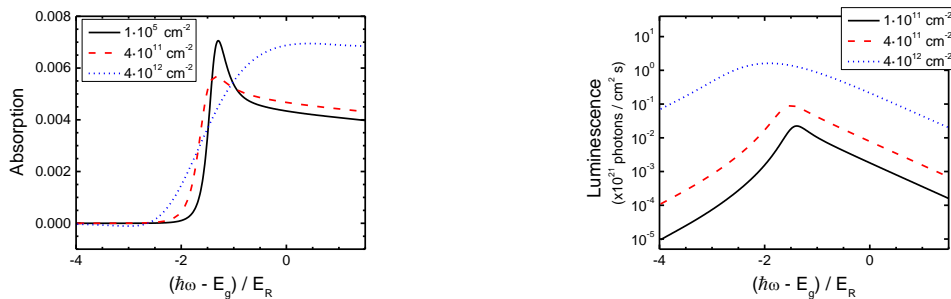


Fig. 2. Absorption (left panel) and luminescence (right panel) spectra shown for three values of density of photo-excited carriers.

The normal incidence absorbance and luminescence spectra are calculated from the QW optical susceptibility under the assumption of quasi-thermal equilibrium. Figure 2 shows the absorbance and

luminescence spectra (summed over scattering in-plane directions and polarization states) at three different values of the photo-excited carrier density. It is seen from Fig. 2 that a negative absorption (optical gain) near the absorption edge appears at high carrier surface density.

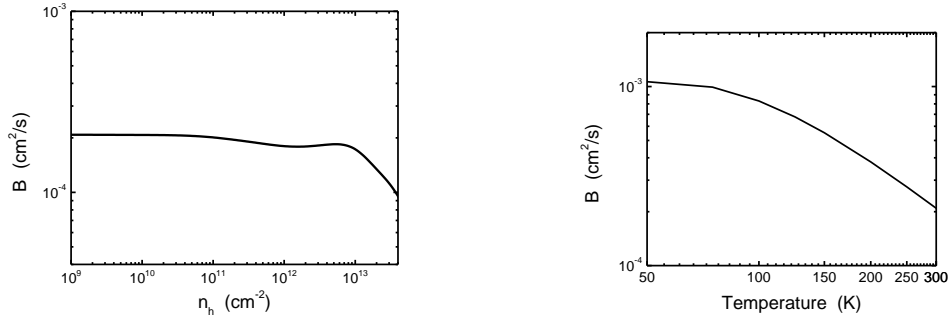


Fig. 3. The recombination coefficient B . It is shown in the left panel at room temperature as a function of the photo-excited hole density (in surface units) and in the right panel as a function of temperature at $n_h = 10^5 \text{ cm}^{-2}$.

The recombination coefficient is obtained from the integrated photo-luminescence, $B(n_h, T)n_e n_h = \int d\omega R(\omega)/2\pi$ [2]. It is shown in the left panel of Fig. 3 at room temperature as a function of the photo-excited hole density (in surface units) and in the right panel of the same figure as a function of temperature. The rise of the radiative recombination rate at high photo-excitation density is due to the strong screening of the polarization electric field.

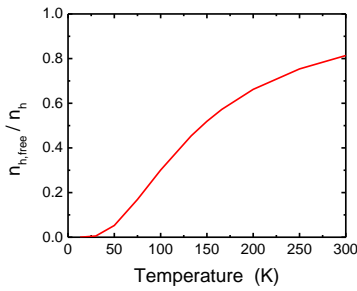


Fig. 4. Hole ionization ratio vs. temperature for low density (10^5 cm^{-2}).

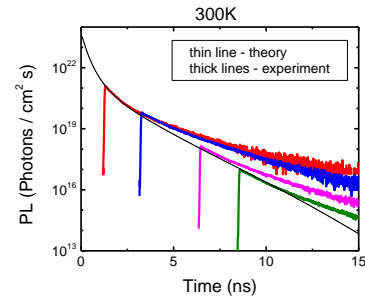


Fig. 5. Comparison of theoretical and experimental results for time resolved photoluminescence.

The ionization ratio ($n_{h,free}/n$) is shown in Fig. 4. Where $n_{h,free}$ is that part of the holes which are not bound into an exciton. Away from the zero-density, zero-temperature limit, when the exciton peak acquires a sizable width, the definition of this “free-plasma” density is not free of ambiguities. Here we estimate it to be equal to the density of a hypothetical non-interacting hole gas at the same respective chemical potential as the interacting hole plasma in our theory. It can be seen that the number of excitons decreases as the temperature increases. The number of excitons at room temperature is lower than might be expected due to screening from donor electrons and the separation of the electron and hole due to the polarization field.

Using the calculated radiative lifetimes we obtained the time dependence of the photoluminescence. The results are compared to time dependent photoluminescence decay experiments performed by G. A. Garrett et al. [3], in Fig. 5 the theoretical model has excellent agreements with the initial fast decay seen in the TRPL experiments. This model can aid in the design of III-N MQW devices.

References

- [1] N. H. Kwong et al, “Self-consistent T-matrix theory of semiconductor light-absorption and luminescence,” *Phys. Rev. B* 79, 155205 (2009).
- [2] G. Rupper et al., “Theory of laser cooling of semiconductor quantum wells,” *Phys. Stat. Sol. (b)* 245, 1049 (2008).
- [3] G. A. Garrett et al., “Evaluation of AlGaN-based deep ultraviolet emitter active regions by temperature dependent time-resolved photoluminescence,” *Phys. Stat. Sol. (c)* 7, 2390 (2010).